# Improving Protein Stability Analysis in Thermal Proteome Profiling: A Correlation-Based Aggregation Approach

Thesis

Presented in Partial Fulfillment of the Requirements for the Degree Master of Science in the Graduate School of The Ohio State University

By

Melanie Chen

Graduate Program in Public Health

The Ohio State University

2025

Thesis Committee

Brian C. Searle, Advisor

Michael Pennell, Committee Member

Damien Wilburn, Committee Member

Abstract

Thermal proteome profiling (TPP) is a powerful method for studying protein stability and interactions by measuring thermal denaturation profile. It is based on the principle that proteins denature and become insoluble when subjected to heat. TPP can be used to investigate melting temperature profile shifts. By studying that shift we can investigate protein chaperones. Protein chaperones play an essential role in helping protein folding, assembly and quality control. An alternative method for cell lysis and an optimized TPP workflow were needed to accurately collect data. Using ethanol dry ice slurry proved to efficiently lyse cells.

In this study we aimed to investigate GRP94 and BiP and their melting temperature profile. Based on literature, GRP94 is more selective than most endoplasmic reticulum (ER) chaperones which was confirmed with data in this study. Having an accurate melting temperature is important as it affects the melting temperature shift. Current methods utilize the top three method where the top three most intense peptides are aggregated into a single curve to determine the melting temperature. A correlation-based aggregation method was investigated in comparison to the top three method to determine if there is an alternative aggregation method. Global analysis of GRP94 and BiP were conducted along with investigations into certain proteins to compare the two methods. By determining the effectiveness of the correlation-based aggregation method,

future research in this area could have an alternative aggregation method that is more flexible and representative of the overall melting temperature profile.

Acknowledgments

I would like to thank the members of the Searle lab for their support in my research and the Pelotonia Institute for Immuno-Oncology for providing the space for my study. I would also like to acknowledge my advisor, Dr. Brian Searle, for providing guidance and support throughout this process, I have learned a lot. Lastly, I would like to give special thanks to Nathan for his unwavering support throughout this process, Kuma, Hinata, Yuki, and Haru for their comfort, and my family for being just a call away when I needed them.

Vita

2016-2021…….. B.S. Chemistry, John Carroll University

Fields of Study

Major Field: Biomedical Informatics

Table of Contents

List of Tables

List of Figures

# Chapter 1: Introduction

## 1.1 Thermal Proteome Profiling

Thermal proteome profiling (TPP) is based on the principle that proteins denature and become insoluble when subjected to heat. Originally developed to detect drug targets within cells, this technique provides insights into protein interactions. In a typical TPP experiment, cells or lysates are subjected to a range of temperatures, causing proteins to denature at melting points. These samples are then analyzed, allowing for the generation of melting curves for different proteins. This approach enables possible assessment of protein-protein interactions and the effects of post-translational modifications on protein stability (17). These curves can provide information on protein-protein interactions and drug interactions, enabling the assessment of drug-target engagement (13), and allowing for proteome-wide thermal change relying on the sensitivity of mass spectrometry. One of the significant challenges in TPP is the identification of protein substrates and the accurate analysis of the melting curve. Data analysis strategies have been developed to improve the sensitivity and accuracy of TPP experiments, addressing issues such as aggregation of data at the peptide level and the impact of peptide intensities on melting temperature calculations.

Some methods sum proteins at a peptide level and some at a protein level. The aggregation method can affect the results, as it determines which peptides and proteins

will be included in the dataset for analysis. Finding a method that suits TPP analysis is crucial as different intensities of peptides can shift the melting temperature and give different results.

TPP relies on fitting protein denaturation curves to sigmoidal functions to estimate melting temperature and infer protein stability or drug interactions. While there are several sigmoidal models that exist, the 4-parameter Hill function has emerged as the gold standard due to its flexibility and biological relevance. The Hill function is a model used to describe sigmoidal curves and is commonly applied in biochemistry and systems biology. It quantifies the relationship between the concentration of a ligand and the receptors (23). The Hill function is.

$$f(x) = \frac{1}{1 + (\frac{EC_{50}}{[A]})^n}$$

This is reparametrized where $EC_{50}$ is replaced with $T_m$ and [A] with temperature and n being the Hill coefficient. However, alternative sigmoidal functions such as the 2-parameter function and 3-parameter logistic model have been explored in other studies, each with advantages and limitations.

The 2-parameter model assume symmetric denaturation around the melting temperature. The equation is.

$$f(T) = \frac{1}{1 + e^{(T_m - T)/k}}$$

Where Tm is the melting temperature and k is the slope factor. The symmetry assumption often fails for multi-domain proteins or complexes which leads to inaccuracies (7). The symmetry around melting temperature means that the denaturation curve has identical steepness in the pre- and post-transition regions. This symmetry is due to the function depending only on the melting temperature and the temperature leading to a mirrored profile before and after the melting temperature. The reason it fails for multi-domain proteins is due to them often having non-symmetric denaturation. Multi-domain proteins have non-symmetric denaturation because domains unfold at different temperatures. The overall domain structure matters even if we are only investigating the melting temperature because the melting temperature would summarize the overall stability of that protein. Forcing a symmetric fit to asymmetric data can introduce noise and cause a reduction in accuracy.

The logistic function is a 3-parameter sigmoidal model that is a middle ground between the 2-parameters and Hill function with 4-parameters. Like the 2-parameter function, the logistic model with 3-parameters is also symmetric around the melting temperature. The logistic function offers slight improvements by decoupling the slope parameter from temperature units, providing better slope steepness values. Decoupling refers to separating linked parameters to get more interpretable and biologically meaningful results (26). The logistic function reformulates the exponent to isolate k from temperature dependence using the equation:

$$f(T) = \frac{L}{1 + e^{-k(T - T_m)}}$$

Now k is directly scaling with the steepness meaning that a higher k value would result in a sharper slope, it is also unitless which would allow for more direct comparison across datasets. Decoupling matters for TPP because unitless k values would allow pooling data to be easier if different temperature increments were used.

The Hill function can perform better than other methods because it can account for baselines. Baseline refers to the signal levels at the extreme ends of the temperature gradient where proteins are fully folded at lower temperatures or fully denatured at higher temperatures. These baselines are important because data do not usually reach the idealized 0% or 100% solubility due to experimental noise or biological complexity. The Hill function is also to model baselines with different plateaus like the upper and lower plateau where proteins are fully folded or fully denatured. The parameters are set by the upper plateau, lower plateau, melting temperature, and the Hill coefficient. The parameters are adjusted to minimize residuals which is the difference between data and fitted curve. Some constraints are put in place where the upper baseline would be greater than the lower baseline. The melting temperature is found where the intensity is halfway between the lower and upper plateaus. Using software, the parameters are then optimized by minimizing the sum of squared errors between the predicted and the measured data. For quality control, the R-square is used to find good fits. If it indicates a bad fit, then it may require better initial values of the parameters. The fitted results will then give what the melting temperature is along with the Hill coefficient. Both the 2-parameter function and logistic function have fixed structures that assume that the proteins the fully folded at

0% or fully denatured at 100%. And as mentioned before, proteins often do not have those idealized values.

The assumption of fixed baselines of 0% and 100% is linked to the symmetry of denaturation curves. The 2-parameter function and logistic function assume that the baselines are fixed where 0% of proteins are folded at high temperature and 100% of proteins are folded at low temperature. This means that at high temperature the protein is completely unfolded and at low temperature the protein is completely folded. However, proteins often are not completely folded or folded so the forced symmetry of that assumption can introduce bias as proteins have residual solubility. Hill function allows for the baselines to be adjustable if needed thus breaking the assumed symmetry and the fixed baselines that can capture protein complexity and fit multi-domain proteins better.

## 1.2 Current Methods

Most methods use the TPP R package from Bioconductor (5) which is designed to analyze TPP data (Table 1). It handles the data from label-free and isobaric labeling experiments and models' protein thermal denaturation curves using the sigmoidal function and provides diagnostic plots and statistical methods to assess data quality. The input data usually consists of protein intensities measured across a temperature gradient; the configTable specifies sample condition, while dataPath contains raw protein quantification data, with dataNorm accounting for systemic biases and ensuring comparability. The identified proteins with altered stability are stored in the results.

A study of the thermostability of Escherichia coli (E. coli) proteins in vivo provided insights into protein complexes and metabolic pathways (17). They used TPP in combination with tandem mass tags (TMT), which enabled the detection of changes in protein thermostability under different conditions. The protein identification and quantification were performed using liquid chromatography coupled with tandem mass spectrometry with TMT-based multiplexing. Peptides were fractionated and the data were processed with IsobarQuant, while peptide identification was conducted using Mascot 2.4 against the E. coli UniProt database. The variance stabilization normalization was applied to the raw data before melting curves were fitted using the TPP R package. This transforms the data to make variance independent of mean intensity to ensure equal weighting of all proteins. For this experiment they needed to compare melting curves across proteins fairly and enable clustering of co-melting complexes. Without variance stabilization, a protein complex with high abundance and low abundance might cause uneven noise. Protein complexes were analyzed using a thermal proximity coaggregation approach to assess if the complex subunits have co-melting behaviors. The top three most intense peptides for each protein were identified and aggregated for further analysis. The Euclidean distance was measured between the melting curves of complexes and was calculated to determine clustering patterns. This method demonstrated that TPP can provide a robust method for studying protein stability in vivo that offers application in drug target identification and protein-protein interactions.

The study by Becher (3) employed a two-dimensional TPP approach combined with chemo proteomics to identify protein targets. The method provided insights into off-

target interactions. TPP was performed to assess dose-dependent thermal stabilization in response to Panobinostat treatment. To confirm the direct binding of the treatment to its targets, an affinity enrichment-based chemo proteomics approach was used. After the LC-MS/MS analysis, raw data were processed to ensure quality control and normalization. Protein identification was performed using Mascot 2.4 against a customized version of the International Protein Index (IPI) database. The peptide spectrum matches were filtered using the criteria: Mascot ion score larger than 15, signal-to-background ratio larger than 4, and signal-to-interference ratio larger than 0.5. Reporter ion intensities were extracted and corrected for isotope purity and interference using a bootstrap algorithm. The algorithm corrects for isotope impurities and interference in TMT reporter ion quantification. The approach randomly samples the MS/MS data multiple times in iterations and calculates correction factors for each TMT channel based on distributions. Then it averages results to derive purity-corrected intensities. The intensity values were also normalized to correct for batch effect since TMT-based quantification was used. To determine the melting point, quality control steps were applied where the R-squared of the curve fit had to be larger than 0.8, the plateau of the curve had to be less than 0.3, and the steepest slope of the curve had to be less than -0.06. These helped remove poorly fitted curves and ensure that most proteins have fully denatured.

In Yin's study (24), MS/MS spectra were searched using Mascot against the UniProt database with a taxonomy filter of '9606', which refers to Homo sapiens, was supplemented with common-containing proteins and concatenated with all the decoy

sequences. Search parameters allowed for trypsin cleavage with up to two missed events and a precursor ion tolerance of 50 ppm. Peptide spectrum matches (PSMs) were filtered at a false discovery rate (FDR) of 5% at the peptide level and 2% at the protein level using linear discrimination. TMT reporter ions were quantified using an in-house software package, Mojave (22) by identifying the highest peak within 20 ppm of theoretical reporter mass windows and correcting for isotope purities. Those quantified were filtered to retain those with a total TMT reporter ion intensity greater than 50,000 and an isolation specificity above 0.7 before being summarized at the protein level. Protein abundance ratios across treatment groups were calculated as the percentage of the total TMT signal for each protein. Aggregation happens at a peptide level first, where TMT reporter intensities are assigned to PSM, then into the protein level using the summarization method. Having a set of thresholds for peptides is helpful in retaining only peptides that can be used in the analysis process.

In Franken's study (7) the melting curves were fitted to the fold changes of each protein using the equation,

$$f(T) = plateau + \frac{1 - plateau}{1 + e^{\frac{1}{T} - b}}$$

Where T is the temperature and a, b, and plateau are constants. The melting temperatures of the protein were given by the temperature at which the value of the

melting curve is 0.5. The model fitting was performed by non-linear regression using the nls function in R, which is different from other methods using the TPP R package. Median melting temperatures were reported if proteins were quantified with at least two unique peptides across replicates. In the 2D-TPP experiments, proteins were evaluated across different compound concentrations, normalized, and analyzed based on stabilization criteria. Scatter plots visualized stabilization scores to identify significant thermal stability changes.

A mass spectrometry data analysis study was done to assess protein stability and inhibitor effect using TPP (14). The signal intensity was measured across different temperatures and fitted to a sigmoidal curve using a nonlinear least squares approach in R. The melting temperature and slope parameters were determined, and the thermal shifts induced by inhibitors were reported relative to the control. A statistical comparison using ANOVA assessed whether inhibitor treatment significantly altered protein melting behavior. Dose-response curves were fitted using the Hill function (9), determining the melting temperature and Hill coefficients for different inhibitors. MS data were processed using MaxQuant with protein identification based on the UniProtKB database, and quantification was performed using label-free and TMT-based approaches. Melting curves were normalized, and the data were fitted using a four-parameter model for TPP-TR. The outliers were removed, and the final melting points were determined per protein. For TTP-CCR, intensity values were normalized across inhibitor concentration gradients, and dose-response curves were fitted using nonlinear regression. The goodness of fit was assessed using an R-squared value, and filtering criteria were applied to retain proteins

with consistent dose-response behaviors. Using various methods and thresholds for screening peptides may give different results.

Table 1. Method summary of the current methods for TPP analysis.

| References | Method/ Software | Aggregation Level | Screening Thresholds |
|---|---|---|---|
| (7) (17) | TPP R package | Protein level quantification was based on the top three most intense peptides. | Trypsin digestion up to three missed cleavages, peptide tolerance of 10 ppm, MS/MS tolerance of 0.02 Da. |
| (24) | TPP R package | Protein level quantification was done by summing the intensities of all peptides for each protein. | 10 ppm precursor mass tolerance, 0.025 Da product ion mass tolerance, FDR < 1% (peptide and protein level) |
| (4) | nlsM() R package | Peptide level filtering was done before aggregation, and protein level aggregation was done based on protein groups. | 20 ppm precursor mass tolerance initially and then 4.5 ppm precursor mass tolerance, FDR < 1% (peptide and protein level), unmodified counterpart peptides were discarded |

| | | | |
|---|---|---|---|
| (21) | nlme() R package | Peptides that were in top matches in the database were retained and aggregated into protein melting temperatures. | 100 ppm of precursor mass tolerance, 0.5 fragment mass tolerance, and a maximum of one missed cleavage |

In TPP, accurately capturing the melting behavior of a protein is essential for determining its thermal stability and potential interactions. Peptide aggregation strategies often rely on selecting the most intense peptides, however, this approach can introduce biases, as highly abundant peptides may not consistently reflect the protein's overall melting point profile. A correlation-based selection method was explored in our study to improve accuracy. By identifying peptides with the most consistent melting curves, this method reduces the influence of outliers and ensures that the final aggregated curve more reliably represents the unfolding behavior of the entire protein. Only peptides that follow a similar sigmoidal trend are filtered and included, thus reducing the impact of noisy peptides. Aggregating highly correlated peptides produces a smoother and more consistent melting curve as well, which leads to a more accurate hill function fitting curve at the protein level.

### 1.3 Chaperones: GRP94 and BiP

In the context of endoplasmic reticulum (ER) chaperones, TPP has been applied to map their client networks, identify interaction partners, and explore the effects of chaperone-targeting inhibitors. By detecting thermal stability shifts upon chaperone

binding or inhibition, TPP can reveal direct and indirect interactions that can offer valuable insights into protein mechanisms. It reveals direct interactions by detecting target engagement and TPP can identify these shifts by comparing melting curves between treated and untreated samples. It can also reveal indirect interactions by mapping cellular responses. An indirect effect arises when a drug or mutation alters the stability of proteins. TPP has been extensively used to map the interactome of cytosolic HSP90 (19) revealing a network of client proteins whose stability decreased upon drug treatment. One study (10) demonstrated that TPP could identify ER-resident chaperone interactors by measuring protein thermal stability in response to stress conditions, allowing for the detection of protein-protein interactions.

Chaperone proteins play an essential role in maintaining cellular homeostasis by assisting in protein folding, assembly, and quality control. Among them, glucose-regulated protein 94 (GRP94) and immunoglobulin-binding protein (BiP) are two key chaperones located in the ER, where they regulate protein maturation and stress responses (6).

GRP94, an HSP90-like protein located in the endoplasmic reticulum (ER) lumen, shares structural and functional similarities with cytosolic HSP90 proteins, including its ATPase activity (12). However, GRP94 also possesses unique features such as calcium-binding capabilities (25), which are critical given the ER's role as a major calcium storage compartment. Unlike other ER chaperones, GRP94 exhibits a more selective client repertoire (16), although the molecular basis for this selectivity remains poorly understood. Evolutionarily, GRP94 has adapted to manage a distinct set of client proteins

and stress responses compared to HSP90. Its essential functions include facilitating protein folding, assembly, secretion, and antigen presentation, particularly for membrane-bound and secreted proteins. Notably, GRP94 interacts with a smaller and more specific group of substrates compared to other ER chaperones like BiP. While many plasma membrane receptors and secreted proteins do not require GRP94 for proper folding, some rely on its association due to its abundance in the ER lumen, reflecting a functional consequence of its availability.

The earliest identified GRP94 clients came from the immunoglobulin family, where it binds selectively to the variable (V) domain of light chains, in contrast to BiP, which binds both variable (V) and constant (C) domains (18). This shows a more selective clientele for GRP94. Ablation of GRP94 impairs light chain secretion, although studies in mice indicate that serum Ig levels can remain stable in the absence of GRP94, suggesting the existence of bypass quality control mechanisms. Some toll-like receptors (TLRs) also bypass GRP94 dependence, but their depletion leads to compromised innate immune responses to selected pathogens. GRP94 has garnered attention for its role in immunity, particularly through its ability to stimulate T cells and enhance anti-tumor activity. Identified as gp96, GRP94 is a potent stimulator of cross-priming, a process where dendritic cells capture peptides from other cells and present them to T cells, generating antiviral and antitumor responses. GRP94-peptide complexes are internalized by dendritic cells and antigen-presenting cells through receptor-mediated endocytosis, mediated by scavenger receptors. Once internalized, peptides are separated from GRP94 and loaded onto major histocompatibility complex (MHC) molecules, which are

subsequently displayed on the cell surface for recognition by T cell receptors. Despite its established roles in protein homeostasis and immunity, GRP94's client specificity and mechanisms of action remain active areas of research, with potential implications for therapeutic strategies targeting cancer and immune modulation.

BiP, another major ER chaperone, belongs to the HSP70 family and plays a crucial role in protein homeostasis. It interacts with a broad range of misfolded proteins, preventing their aggregation and targeting them for degradation. BiP is a key regulator of unfolded protein response, binding to misfolded proteins under ER distress and signaling protective cellular mechanisms (8). It associates with transmembrane sensors to regulate ER stress responses (15). In contrast to GRP94's selective client interactions, BiP engages in more general chaperoning activities (1). It binds nascent polypeptide chains to prevent premature folding, facilitates the translocation of proteins across the ER membrane, and participates in the degradation of terminally misfolded proteins through ER-associated degradation (ERAD) (11). The cooperative action of BiP and GRP94 ensures proper protein folding and quality control, maintaining ER homeostasis under both normal and stress conditions. Given their critical roles, both GRP94 and BiP serve as potential therapeutic targets in diseases related to protein misfolding, including cancer and immune dysfunction.

We are interested in using TPP to identify potential chaperone clients of GRP94 and BiP. By enabling the study of protein stability and interactions under conditions, TPP provides crucial insights into cellular mechanisms, protein function, and protein-protein interactions. Understanding chaperone proteins through TPP can help elucidate their roles

in disease pathology and therapeutic development. By enhancing the methodologies for analyzing TPP data and improving accuracy and reliability, the insights gained from this could contribute to advancing biomedical research.

# Chapter 2. Methods

## 2.1 Thermal Proteome Profiling

We obtained three sets of samples with a total of 30 samples, including control, GRP94 knockout, and BiP knockouts. All the samples were resuspended in 99% phosphate-buffered saline (PBS), pH 7.4, (Gibco, Catalog Number 10010001, Carlsbad, CA) with HALT (1%) to ensure the cells within the solution were dispersed evenly. We used 90 uL of resuspension buffer for the control set and 100 uL for the treatment sets. Following conventional TPP protocols, we used ten different temperatures as treatments: 37, 40, 43, 46, 49, 52, 55, 58, 61, and 64°C. The heat treatments were performed using a ThermoMixer (Thermo Fisher Scientific) to set to the desired temperatures, and samples were heated to each temperature for three minutes, then the samples were taken off to cool for three more minutes before snap-freezing in an ethanol dry ice slurry. Unlike standard TPP protocols that use liquid nitrogen, we used ethanol/dry ice slurry to perform cell lysis on the cells to ensure the separation of proteins from the cells. The ethanol dry ice slurry was used because we did not have access to liquid nitrogen. The slurry was made using 500 mL of ethanol and enough dry ice to cover the sample vials in an ice bucket. The samples were frozen in the slurry for thirty seconds and then transferred to a thermomixer with a temperature set to 37 degrees Celsius for 1:30 minutes. Samples were kept on ice when they were not being treated with heat or lysed. This cycle was repeated seven times for all samples. Once all the samples had been lysed, they were centrifuged for 30 minutes at 4 degrees Celsius at 20,000 RCF. This separates the non-protein cell

particles from proteins. Once soluble proteins were recovered, a lysis buffer containing 15% SDS was added to each sample after the pellet had been discarded to lyse any remaining cell particles. The samples were then centrifuged again for 8 minutes at 15 degrees Celsius at 8000g. The lower g speed and higher temperatures ensure that SDS does not precipitate at lower temperatures. The samples were then transferred to clean tubes after discarding the cell pellets. Figure 1 shows an illustrated overview of the TPP experiment used for this study.

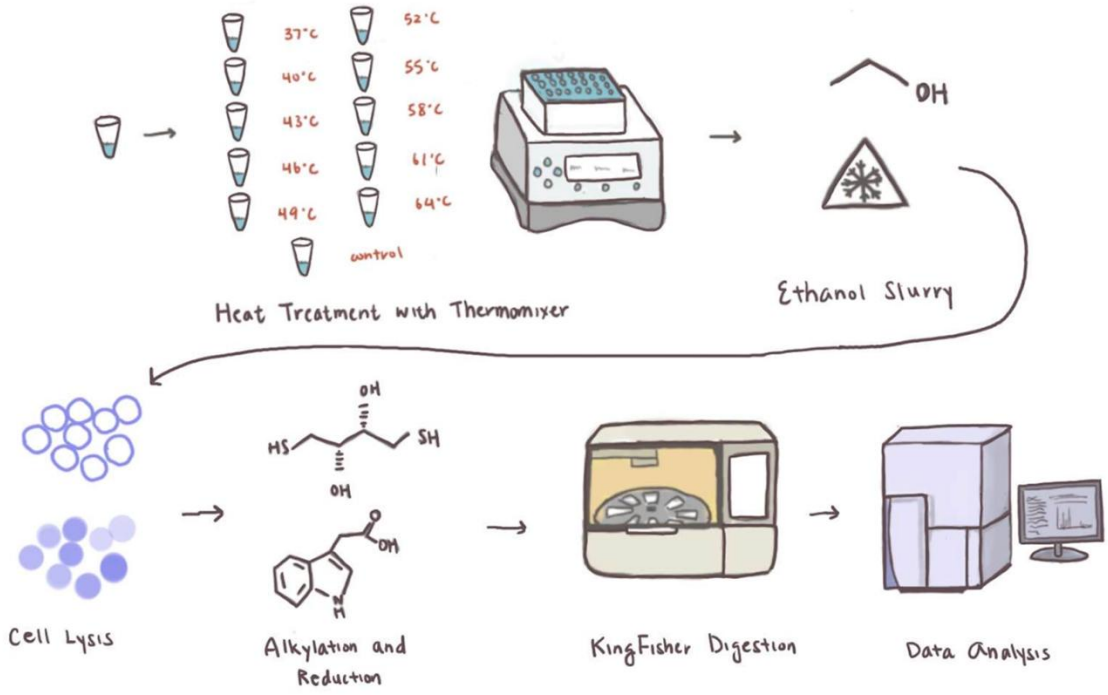


Figure 1. Overall TPP method.

2.2 Ethanol Slurry Cell Lysis Validation

The slurry was set up by adding enough dry ice to cover the sample test tubes with ethanol (Figure 2). Depending on the size of the ice bucket, the amount of dry ice and ethanol may vary. Using imaging and trypan blue dye, cells were seen at various stages.

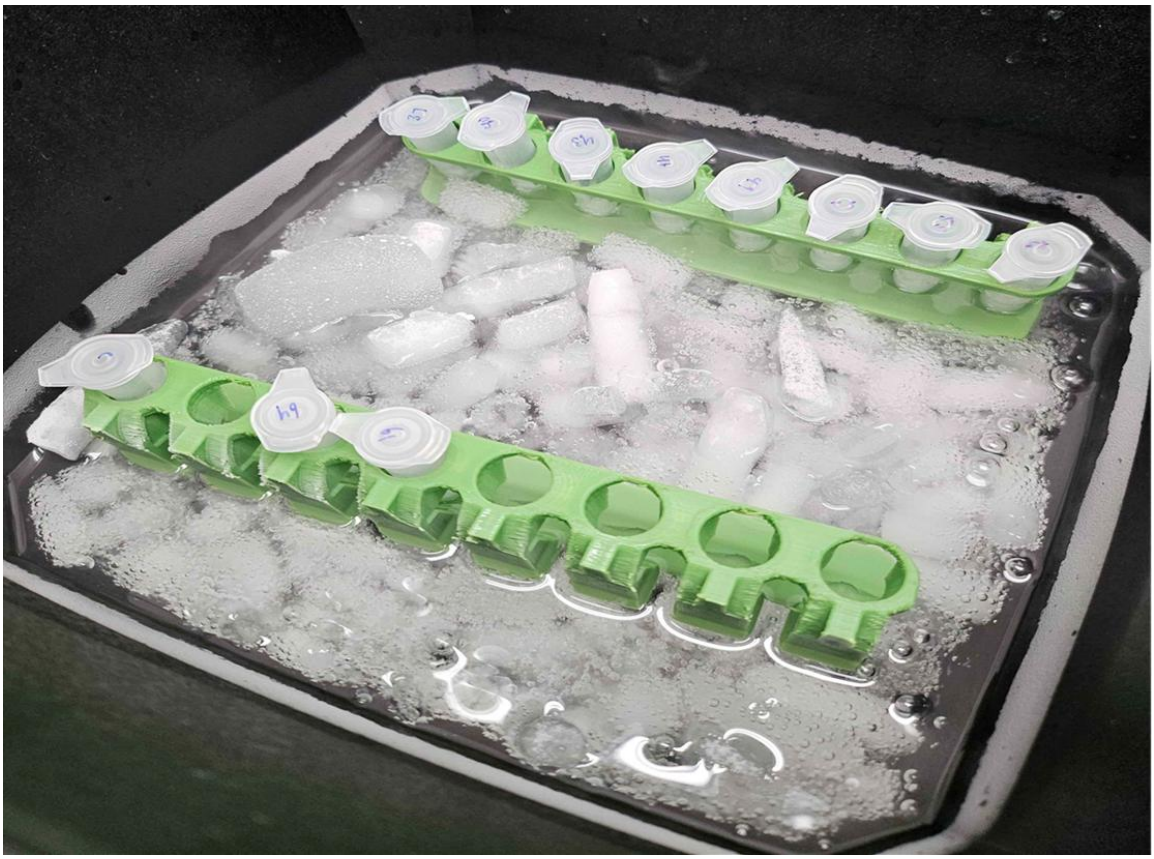

Figure 2. Ethanol dry ice slurry setup.

2.3 Protein Quantification and Mass Spectrometry Sample Preparation

Pierce BCA Protein Assay Kit (Company, Catalog Number, Location) was used for all sets of samples. This method evaluates and determines the total protein concentration in a solution by measuring a color change from blue to purple proportional

to the protein content. Two dilution series were done to all sets of samples: 1:5 and 1:10 (sample: lysis buffer). The lysis buffer used in BCA was diluted more with water with a 1:2 ratio to ensure that the SDS was under 15%. 10 uL of the sample was used for 1:5 dilution with 40 uL lysis buffer. 20 uL of the sample was taken from a 1:5 dilution mixture with 20 uL lysis buffer. 10 uL of each diluted sample was loaded on the 96-well plate with 200 uL of working reagent. Eight BCA standards were used with a blank. We utilized standard protocol standards for this study. The plates were incubated for 30 minutes in a 60°C incubator. The samples were read using a spectrophotometer set to 562 nm. Once the preliminary analysis of the BCA data was done, the samples were alkylated and reduced using DTT and IAA and then quenched.

The protein samples were digested using an automated workflow on the KingFisher (KF) with PAC and hydroxyl beads (2). Eight 96-well KF plates were used. The protein plate contained activated hydroxyl beads with 100% acetonitrile and our protein samples. 100% ACN in the protein plate causes the protein to precipitate. The tip plate contained a KF tip comb. Five wash plates were made with 95% ACN in TEAB and 50% ethanol. The digestion plate contained .05 µg/ uL of trypsin. Each sample was adjusted to have 40 µg of protein based on the BCA data results. This was done by calculating how many µL of the sample are needed and then adding the remaining amount of µL using 50mM TEAB to 100 µL since we used 100 µL of sample per well. We used a 1:4 ratio of hydroxyl beads to protein for the protein plate. The beads were equilibrated twice using 70% ACN. Each plate was placed in the KF, and the protein and bead plates were mixed for ten minutes to allow for the protein to crash out onto the

beads. The beads containing protein were picked up and transferred to the wash plates. After each wash, the protein plate was taken out of the KF and transferred to an incubator at 47 degrees Celsius and incubated for two hours. The plate was covered with a foil microplate. The supernatant was removed after incubation, and 1% formic acid was added to each well. We prepared 30 sample tubes for the supernatants. The plate was placed back into the KF to eluent from the quenching plates. The digestion plate was taken out, and any remaining liquid was pooled together with previous supernatants. The samples were dried down overnight in a speedvac.

## 2.4 Mass Spectrometry Data Acquisition

Liquid chromatography was performed using an Easy-Spray Nano 1200 system equipped with an autosampler for column pickup. The analytical column was a 25-centimeter-long, 75-micron inner diameter column packed with 1.9-micron C18 particles. A trap column with 2 centimeters in length and 75-micron inner diameter packed with 2-micron particles was used for sample loading and initial separation. The mobile phase consisted of Solvent A with 100% water with 0.1% formic acid and Solvent B with 8% ACN with 0.1% formic acid. The gradient used for separation was as follows:

- 0-5 min: 2% solvent B
- 5-15 min: linear increase to 8% solvent B
- 15-95 min: gradual ramp to 44% solvent B
- 95-98 min: increased to 100% solvent B
- 98-103 min: Held at 100% solvent B for column wash

- 103-110 min: re-equilibration at 2% solvent B

The flow rate was maintained at 250 nL/min during the gradient phase and increased to 500 nL/min during the column wash and re-equilibration steps.

Mass spectrometry analysis was conducted using Thermo Exploris with data-independent acquisition (DIA) in both MS1 and MS2 modes. The nanospray ionization (NSI) source operated at 2000 V in positive ion mode with an ion transfer tube temperature of 280 degrees Celsius. The MS1 master scan was acquired in the Orbitrap at a resolution of 60,000, with an automatic gain control (AGC) target of 1000% and maximum injection time set to auto. The mass range spanned m/z 350-1650.

For MS acquisition, 16 m/z isolation windows were applied using higher energy collisional dissociation (HCD) at a normalized collision energy of 27%. MS2 scans were performed at a resolution of 30,000 with an AGC target of 1000% and maximum injection time in auto mode. A staggered window approach was applied for precursor ion selection to ensure optimal coverage of the mass range that improves precursor isolation.

The instrument was calibrated to measure different temperatures during the acquisition to enhance reproducibility. A data spectral library was constructed from six injections that were combined into a pooled dataset. The acquisition was controlled by loop control with multiple isolation windows. A scan was triggered when the signal intensity met a predefined threshold. The normalized collision energy was applied for fragmentation, and isolation windows were adjusted for each method.

Raw DIA-MS data from the instrument were processed using EncyclopeDIA. The raw files were demultiplexed into pseudo-MS2 spectra, and the data were searched against the UniProt FASTA protein database. Demultiplexed refers to the process of separating and assigning mixed spectral data back to their original individual samples. A direct DIA search workflow was applied, generating a spectral library from the sample data.

## 2.5 Data analysis

A min-max normalization was used on all datasets acquired. This method rescales data values to a range between 0 and 1. The minimum value is transformed to 0, and the maximum value of a feature is transformed to 1. This preserves the relationships between original data values. Three datasets were acquired from the study. A control set was used as a reference point to compare to the knockout sets GRP94 and BiP. GRP94 and BiP knockout sets were the treatment sets. The Hill function was used to model protein unfolding transitions that allow for the quantification of binding and stability changes. This function is useful in TPP as it accounts for sigmoidal behavior in protein denaturation. The Hill coefficient provides insight into the binding effects and deviations between the control and the knockout conditions that indicate changes in protein-protein interactions. The parameters derived from the Hill equation, including the melting temperature and Hill coefficient, were used to assess differential stability.

# Chapter 3: Results and Discussion

This section presents the results of the study with details of the validation of the ethanol dry ice slurry method for cell lysis as well as the effectiveness of the correlation-based method compared to the top three methods. A global analysis was also performed to provide insights into melting temperature profiles.

## *3.1 Cell Lysis Validation*

A dry ice ethanol slurry was chosen as an alternative lysing method due to a lack of access to a nitrogen tank. This approach provides a more accessible and cost-effective solution for researchers facing similar constraints. From pre-freeze images, the cells are shown to be fully intact, where the trypan blue dyes the other membrane of the cell. Each cycle is done by freezing the samples in the slurry for thirty seconds and then transferring them to  a thermomixer with a temperature set to 37 degrees Celsius for 1:30 minutes. We evaluated how the cells would look at cycles one, three, and five. At cycle five, the cells are seen to have been lysed with the trypan blue dye, showing that the cell membrane was broken (Figure 3.1). To ensure successful lysing of cells, we have determined that cell lysis at seven cycles with the ethanol slurry will lyse the cells completely. This method not only provides an effective alternative to traditional nitrogen-based lysis but also offers practical solutions for those with limited resources.

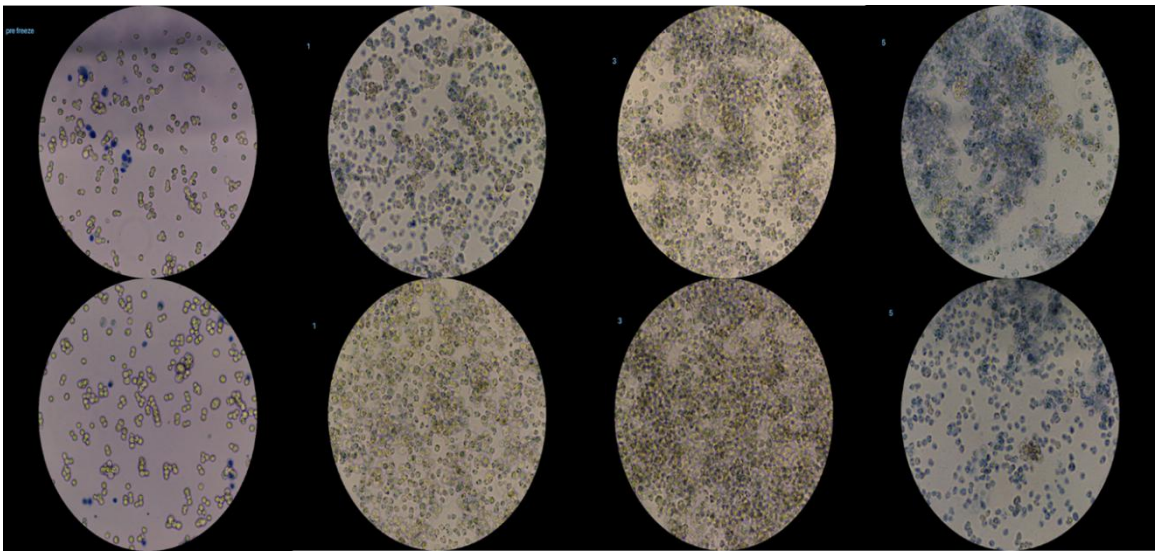

Figure 3. Cell lysis ethanol slurry cycles. Pre-freeze shows intact cell membranes from Trypan blue dye. Cycle one, three, and five are shown, respectively, with cycle five showing that the cell membranes have been lysed, showing the success of ethanol dry ice slurry as an alternative lysing method.

## 3.1Global Data Analysis: Correlation

The first analytical approach aimed to evaluate protein melting temperatures by fitting the peptide intensity values to a Hill function curve. The goal was to ensure a high correlation between the peptide intensity values and the fitted curves, which would enhance the reliability of the thermal stability profiles. The dataset was obtained and checked to ensure it contained the required temperature-dependent intensity values. The objective of this approach was to estimate the melting temperatures of proteins by analyzing the intensities of the peptides using correlation. Peptides were fitted to a Hill function curve while aiming for a high correlation between the observed intensities and the fitted curves. Correlation measures the strength and direction of the linear relationship

between two variables. R-squared is the coefficient of determination, which indicates how well the fitted curve explains the variability in the data. Correlation and R-squared are mathematically related, but correlation reflects the linear association between two variables, while R-squared indicates how much variability can be explained by the model. Correlation alone was deemed sufficient for this analysis as it directly measures the relationship. A strong correlation would enhance the reliability of the thermal stability profile.

Peptides were filtered based on their correlation with the Hill function fit with this dataset. The purpose is to ensure only peptides with reliable melting behavior contribute to protein stability profiles. A low correlation implies that the peptide's solubility does not follow the predicted pattern. This can be due to noise or peptides from different domains melting at different temperatures. Filtering using correlation can provide a more reflective overall melting temperature profile. Based on the distribution of peptide correlation, it was determined that 0.7 would be the criterion used to filter peptides (Figure 4a). In cases where no peptides meet the 0.7 threshold, the threshold will be reconsidered based on the distribution histogram. The highest correlation for each protein was recorded, and the number of proteins with at least one high correlation peptide was determined. A histogram was generated to visualize the distribution of correlation values across all peptides as well as the maximum correlation per protein (Figure 4b). Those with 0.7 or above correlation peptides were aggregated per protein by summing the intensities at each temperature. Summing the intensities that fit the threshold helps smooth out random fluctuations and gives a more representative profile rather than being

dominated by individual peptide variability. This allowed for a more representative thermal stability profile for each protein rather than relying on peptide data points. The aggregated data were then used to fit the melting curves and estimate the melting temperature (Figures 4c and 4d). This was done by interpolating the normalized intensity value and determining the temperature at which the signal intensity dropped to 50%.

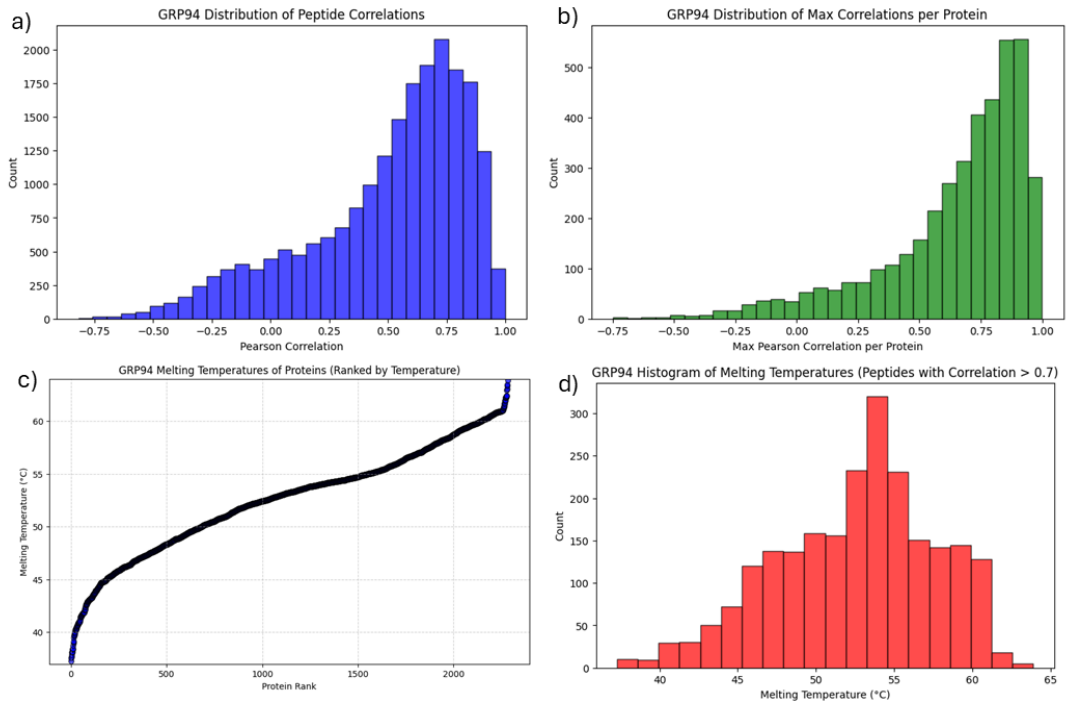


Figure 4. GRP94 global data analysis using correlation aggregation-based method. a) Distribution of peptide correlation that determines the correlation threshold. b) Distribution of max correlation per protein. c) GRP94 melting temperature of proteins ranked, showing the trend of melting temperature globally. d) GRP94 histogram of melting temperature using a correlation of 0.7 or above peptides.

To ensure biologically relevant results, only melting temperatures within the range of 37 degrees Celsius to 64 degrees Celsius were considered and recorded. The

final dataset was sorted by melting temperature, ranked, and visualized using a scatter plot to illustrate the distribution of protein melting temperature. The proteins were ranked to ensure clarity when displaying the data. A histogram was also created to show the frequency distribution of melting temperatures for peptides with high correlation values.

## 3.2 Global Data Analysis: Top Three Peptides

An alternative approach was used to evaluate protein melting temperatures by aggregating the top three most intense peptides for each protein (20). This method was applied as a benchmark to compare with the correlation-based peptide filtering approach, as the top three aggregation methods are commonly used in TPP studies. The dataset was first reviewed to ensure that it contained the necessary temperature-dependent intensity values. This method was used to compare it to the correlation-based peptide filtering approach. The top three peptide aggregation methods are commonly used in TPP studies, making it a relevant benchmark for comparison. This was done to assess whether the correlation-based method provided a more accurate or representative thermal stability profile.

For each protein, the peptide intensities were sorted in descending order at every temperature condition, and the top three peptides with the highest intensities were selected and summed at each temperature to generate an aggregated signal profile. The aggregated data was used to fit the melting curves and estimate the melting temperature. This was done through linear interpolation of the normalized intensity values,

determining the temperature at which the signal dropped to 50% of its maximum value. To ensure biologically relevant results, only melting temperatures within the range of 37 degrees Celsius to 64 degrees Celsius were recorded. The melting temperatures were plotted using a scatter plot and ranked by protein, just as above with the correlation aggregation-based method (Figure 3.3a). A histogram of the melting temperature was plotted and revealed that the melting temperature profile for this method showed more variation and was more scattered when compared to the correlation-based aggregation method (Figure 5).

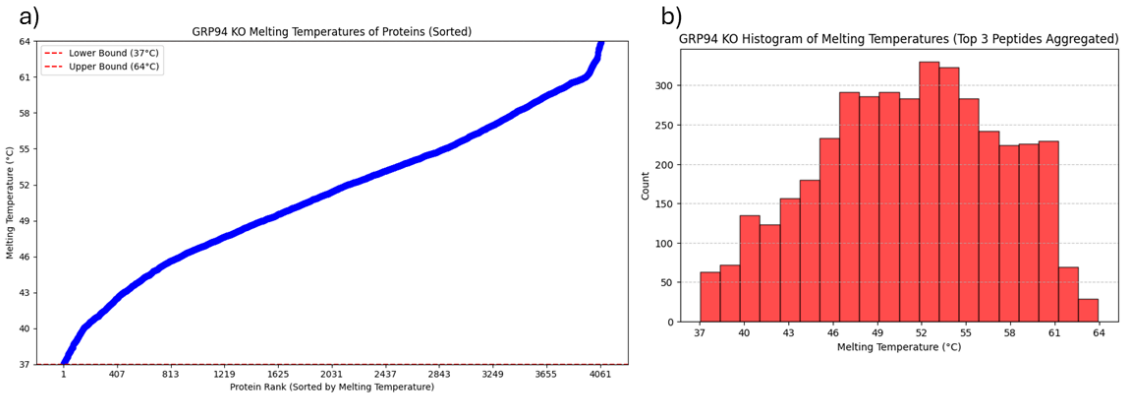


Figure 5. GRP94 global data analysis using top-three aggregation method. a) GRP94 melting temperature profile ranked by protein. b) The GRP94 histogram of the melting temperature profile shows a more evenly distributed distribution.

## 3.3 Protein Analysis

Assessing the algorithmic approach with PLEC, TLN1, EMC29, PYR1, and GRP75

The proteins were analyzed to evaluate differences in their melting temperatures between control and treatment/knockout conditions to assess the algorithmic approach. The proteins were chosen based on the number of peptides and some of these proteins had higher peptide counts as well as lower peptide counts. Having proteins with high and low peptide counts allowed us to explore how the method would perform. As an exploration of the correlation-based aggregation method these proteins were not chosen due to biological significance but rather as examples to compare the two methods. Correlations were calculated using predicted and experimentally measured curves for the y-axis while melting temperature values were used for the x-axis. To assess whether a distinction in melting temperatures existed between the control and treatment groups, clustering analysis was performed using MiniBatch K-Means that minimizes the sum of squared distances between data points and their respective cluster centers. The analysis used two key variables for each peptide: melting temperature derived from the Hill function and the correlation value. p

The clustering process involved an initial estimation of cluster centers, followed by iterative assignment of data points to the nearest cluster based on Euclidean distance. The cluster centers were then recalculated as the mean position of all data points within each cluster. This iterative process continued until the cluster centers stabilized. Cluster determination was based on spatial distribution and data characteristics, with distance metrics guiding grouping decisions and silhouette scoring validating cluster quality. The number of clusters was set to two to three clusters as the MiniBatch allowed for a smaller number of clusters.

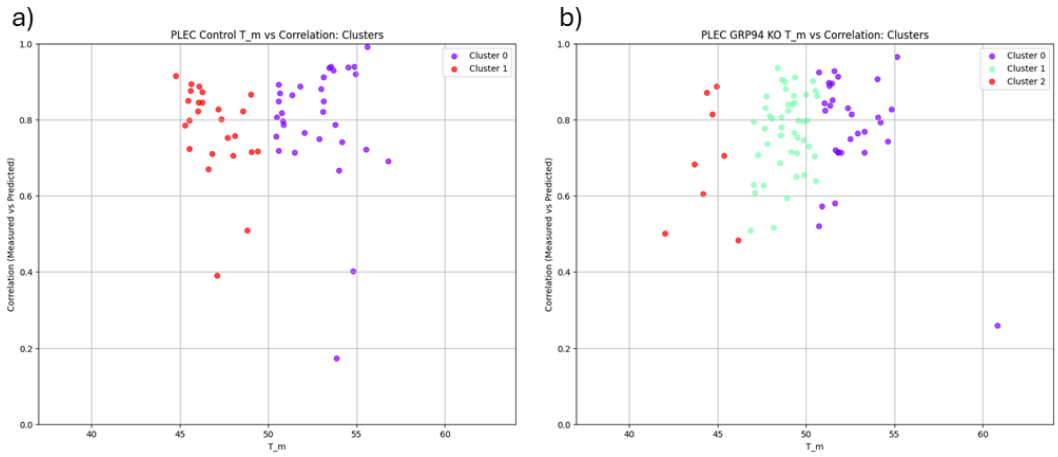


Figure 6. Correlation cluster analysis of PLEC protein. a) PLEC control set. b) PLEC GRP94 knockout set.

From this clustering analysis, distinct melting temperatures were observed (Figure 6). The PLEC control set exhibited a clear melting temperature of around 55°C, characterized by a high correlation within that cluster (Figure 6a). In contrast, the PLEC GRP94 knockout set showed a reduced melting temperature of approximately 48°C, suggesting a shift in protein stability under knockout conditions (Figure 6b). These findings highlight the impact of GRP94 on PLEC thermal stability and underscore the effectiveness of clustering methods in identifying melting temperature variations. TLN1 showed a similar result where the melting point profile shifted after the knockout of GRP94 (Figure 7).

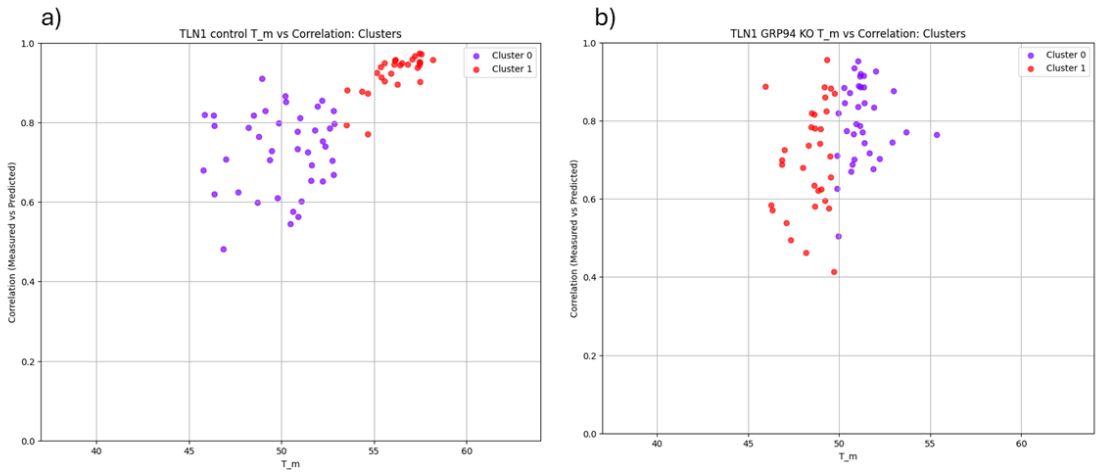


Figure 7. Correlation cluster analysis of TLN1 protein. a) TLN1 control set. b) TLN1 GRP94 knockout set.

Once the peptides were filtered by using correlation as a criterion, an aggregated curve was generated to fit a Hill function. PLEC and TLN1 both used 0.9 correlation as a criterion to filter the peptides. The correlation threshold was changed to accommodate the number of peptides for these proteins. The threshold change is manual and would depend on how the distribution looks for each dataset and protein. These proteins had a higher number of peptides overall and within the 0.9 correlation range. Using that as a threshold ensures that those with high correlation are captured for a more accurate representation of the melting temperature profile. The top three methods were employed as well to compare the methods (Figure 8). The correlation-based aggregation method showed a better Hill function curve fit with the melting temperature around 50°C as discussed above for PLEC (Figure 8a). The top-three method showed a steeper Hill function curve fit with a melting temperature closer to 55°C (Figure 8b). When compared to the

correlation aggregation method, the top-three aggregation method showed a less desirable Hill function fit. Protein TLN1 also showed comparable results when comparing the correlation-based method to the top-three method (Figure 8c and Figure 8d). By using the correlation-based aggregation method the curve showed a better Hill function fit that is more representative of the melting temperature profile.

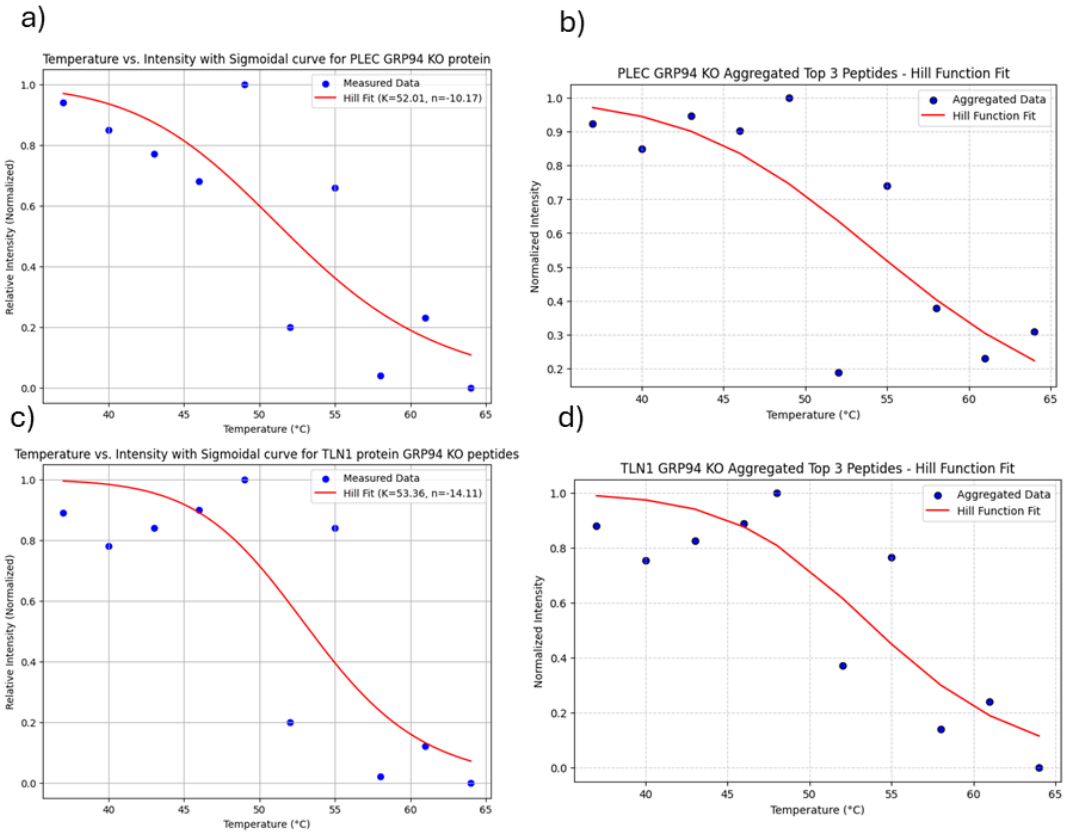


Figure 8. Aggregated peptide protein Hill function curve fit of PLEC and TLN1 from GRP94 knockout dataset. a) PLEC protein Hill function curve using correlation-based aggregation method. b) PLEC protein Hill function curve using top three method. c) TLN1 protein Hill function curve using correlation-based aggregation method. d) TLN1 protein Hill function curve using top three method.

ECM29 protein analysis was done in an analogous manner. The protein was taken from the GRP94 knockout dataset. Using the clustering analysis, the correlation clusters showed melting temperature for the protein at around 50°C (Figure 9a). Compared to the control of ECM29, where the melting temperature is around 55°C, there is a clear shift in the melting temperature profile (Figure 9b). The control dataset of EMC29 showed peptides with a high correlation, while the GRP94 dataset of EMC29 had a more evenly distributed peptide correlation range. There is a noticeably clear shift in the melting temperature profile.

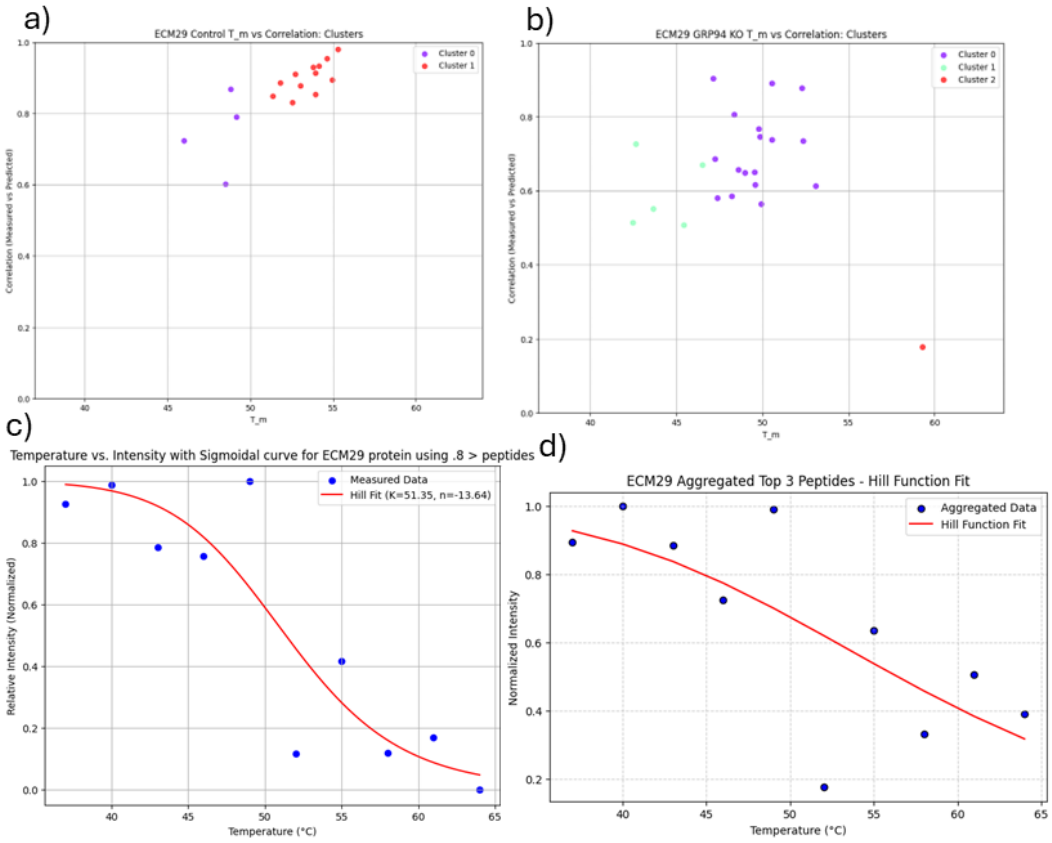


Figure 9. Protein ECM29 analysis. a) Clustering analysis of the control set to determine correlation and show a general trend of melting temperature. b) Clustering analysis of the GRP94 knockout set to determine correlation and show a general trend of melting temperatures. c) Hill function curve fit using correlation method with correlation threshold of 0.8 or above. d) Hill function curve fit using the top three method.

Due to the smaller size of peptides in ECM29 protein 0.8 was used as a criterion for filtering peptides to aggregate into the new curve. The aggregated data fit with the Hill function and showed a sigmoidal curve with a melting temperature of 51.3°C (Figure 9c). To compare with our method, we also used the top-three aggregation method to visualize the data. The top 3 methods showed a less desirable Hill function fit where the

melting temperature was at 56.4°C (Figure 9d). This method yielded a less desirable Hill function fit, further supporting the correlation-based approach as the more reliable method for capturing stability changes.

PYR1 and GRP75 proteins were analyzed using the BiP knockout dataset. The control set of PYR1 showed a melting temperature of around 55°C (Figure 10a). PYR1 BiP knockout clusters have shown a melting temperature of around 50 degrees Celsius (Figure 10b). PYR1 had several peptides within the higher correlation range, so 0.85 was selected as a filter for aggregation for the correlation method. The correlation method and the top three methods were used to analyze PYR1 as well (Figures 10c and 10d). The melting temperature profile showed a shift when looking at the clusters. Based on the correlation-based aggregation method the Hill function curve displayed a better sigmoidal curve.

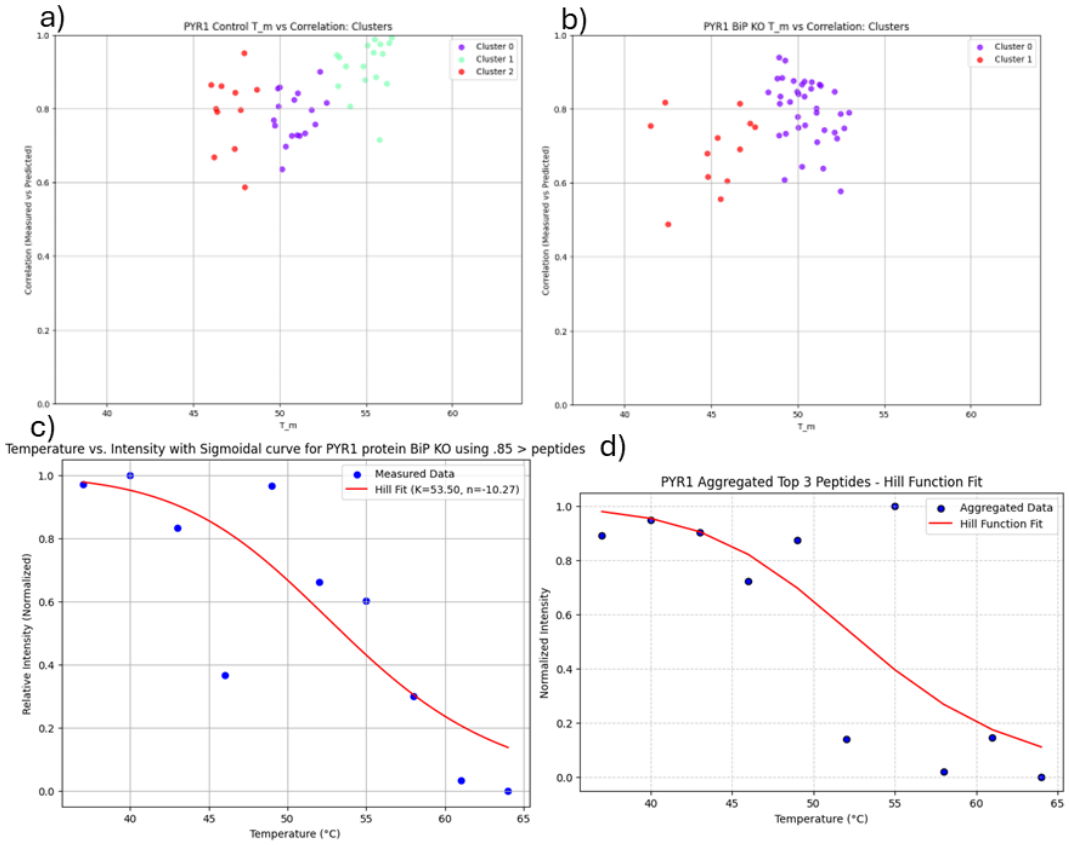


Figure 10. PYR1 protein analysis. a) Control cluster analysis. b) BiP knockout cluster analysis. c) Hill function curve fit using correlation-based aggregation method. d) Hill function curve fit using the top-three method.

GRP75 was analyzed in the same way with 0.7 as a filter for peptide aggregation due to the amount of the peptide being on the lower end. For the control set, the melting temperature was around 53°C (Figure 11a), and for the BiP knockout set the melting temperature was around 47°C (Figure 11b). The correlation method and the top three methods were used (Figures 11c and 11d).

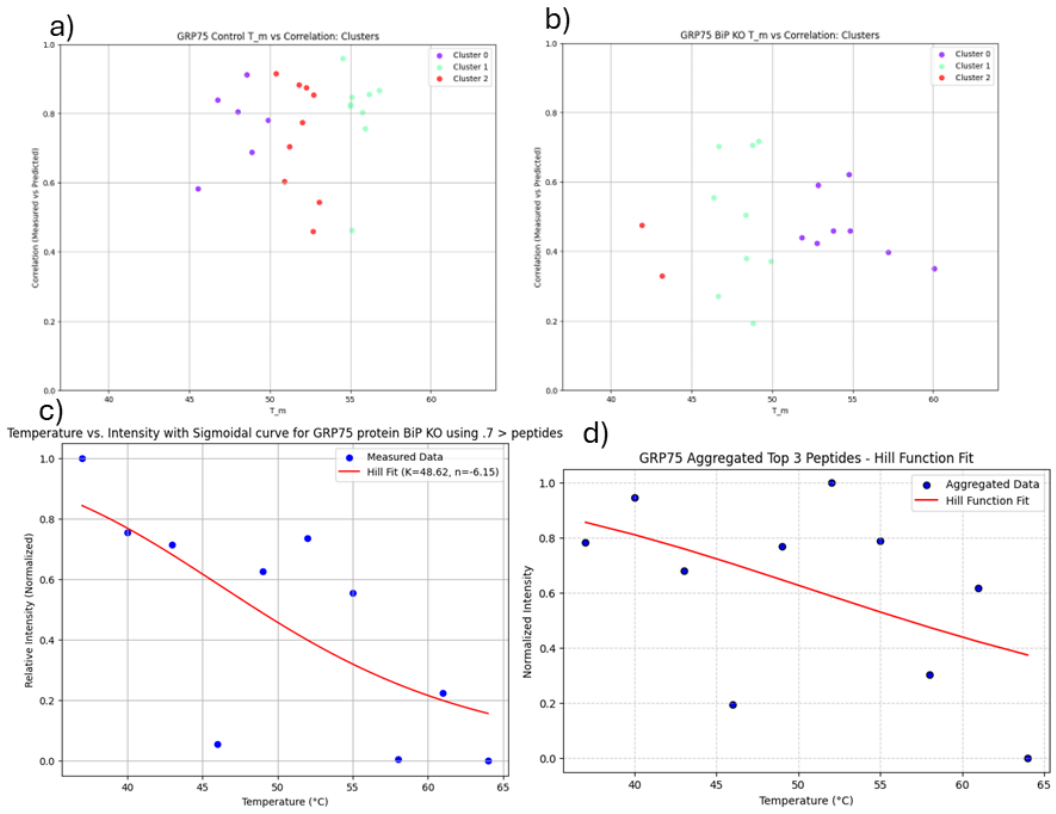


Figure 11. GRP75 protein analysis. a) Control cluster analysis. b) BiP knockout cluster analysis. c) Hill function curve fit using correlation-based aggregation method. d) Hill function curve fit using the top-three method.

## GRP94 and BiP Global Analysis of Melting Temperatures

This analysis aimed to compare the delta melting temperatures of proteins within the GRP94 and BiP datasets, relative to the control set. The goal was to determine whether the presence of GRP94 or BiP induces significant changes in protein stability and how they differ between the datasets. The delta temperature was measured by subtracting the melting temperatures of the control set from the treatment sets. To

visualize the results and distribution of the delta temperatures, an overlapping histogram was generated showing the GRP94 and BiP datasets (Figure 12). BiP dataset showed a broader distribution in the direction of negative delta melting temperatures. A negative delta melting temperature would indicate that the treatment dataset had a lower melting temperature than the control set. Based on the literature, GRP94 is observed to have a more selective clientele (16), which is confirmed with our data.

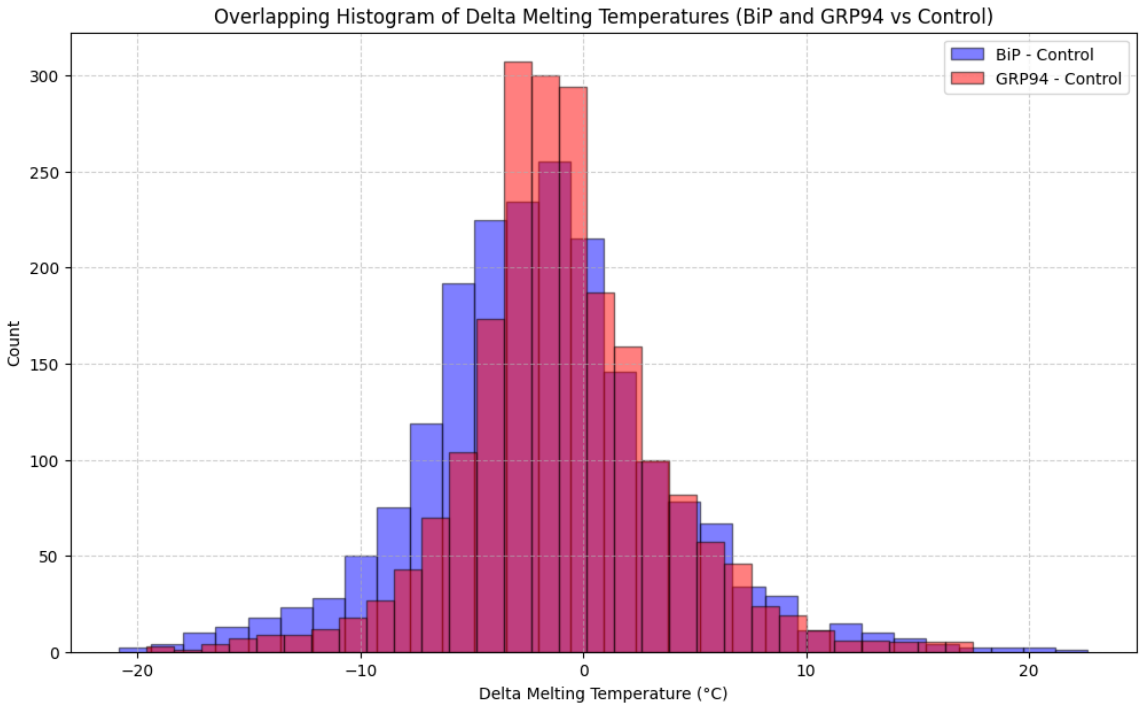


Figure 12. Histogram of delta melting temperature from GRP94 and BiP datasets relative to the control set.

# Chapter 4: Conclusion

The results of the TPP experiment presented reveal critical insights into the behavior and stability of proteins under heat stress. The melting curves generated from the analysis demonstrate the thermal stability of various proteins and their interaction, highlighting the influence of peptide selection and aggregation strategies on the final thermal profiles. The study's use of correlation-based peptide aggregation instead of relying on intensity-based methods addresses a major challenge in TPP analysis. The challenge is the potential distortion of melting curves by outlier peptides or highly abundant, non-cooperative peptides. This approach successfully reduces noise and provides more reliable thermal stability data, improving the accuracy of protein melting point estimation.

The comparison between conventional intensity-based top three aggregations and the correlation-based method highlights the impact of peptide selection on the final melting curve. Intensity-based aggregation, while it is straightforward, can often lead to biased melting curves due to the dominance of highly abundant peptides. These peptides may not accurately represent the protein's overall thermal stability, especially if they exhibit atypical or inconsistent melting behavior. In contrast, the correlation-based method includes peptides with consistent sigmoidal melting profiles, which reduces the influence of outliers and enhances the overall quality of the fitted melting curve. The approach can lead to a smoother melting curve that improves the reliability of downstream analysis, such as determining thermal shifts and protein-protein interactions. The data also underscore the importance of accurate curve fitting in TPP analysis. The

use of non-linear regression models like the Hill function provides robust curve fitting and reliable estimation of the melting temperature. The improved accuracy in melting temperature determination enhances the identification of protein targets and the detection of thermal stability shifts and changes.

The chaperone proteins GRP94 and BiP analyzed in this study serve as key models for assessing TPP accuracy. Both protein chaperones exhibit distinct melting profiles reflecting their differential stability and client binding properties. The thermal stability global data reveal that GRP94 and BiP maintain their stability across a range of temperatures, but GRP94 shows a more selective clientele, as literature has suggested.

Overall, the findings highlight the importance of peptide aggregation strategies, accurate curve fitting, and robust normalization methods in TPP analysis. The correlation-based aggregation method reduces the influence of noisy peptides and gives a more accurate and consistent melting curve. This methodological refinement has significant implications for the broader application of TPP in drug discovery, protein-protein interactions, and proteome-wide assessments. Additional analysis is needed to confirm the significance of biological interactions. Individual proteins can also be analyzed in more detail in future work.

Bibliography


1 B. Huang, M. Sun, R. Hoxie, J.L.M. Kotler, L.J. Friedman, J. Gelles, & T.O. Street, The endoplasmic reticulum chaperone BiP is a closure-accelerating cochaperone of Grp94, Proc. Natl. Acad. Sci. U.S.A. 119 (5).

2 Batth, T. S., Francavilla, C., Olsen, J. V., & Jensen, L. J. (2019). Protein aggregation capture on microparticles enables multipurpose proteomics sample preparation. *Molecular & Cellular Proteomics, 18*(5), 1027-1035. https://doi.org/10.1074/mcp.TIR118.000857

3 Becher, I., Werner, T., Doce, C., Zaal, E. A., Berkers, C. R., Jost, P. J., & Savitski, M. M. (2016). Thermal profiling reveals phenylalanine hydroxylase as an off-target of Panobinostat. *Nature Chemical Biology*, *12*(10), 908–910. https://doi.org/10.1038/nchembio.2157

4 Berning, L., Bozkurt, S., Seemann, L., Wu, H., Khoudoli, G., & Kessler, B. M. (2023). The Golgi stacking protein GRASP55 is targeted by the natural compound prodigiosin. *Cell Communication and Signaling*, *21*(1), 275. https://doi.org/10.1186/s12964-023-01375-0

5 Bioconductor. (2025). *TPP: Bioconductor Package*. Bioconductor. Retrieved March 19, 2025, from https://bioconductor.org

6 Dollins, D. E., Warren, J. J., Immormino, R. M., & Gewirth, D. T. (2007). Structures of GRP94-nucleotide complexes reveal mechanistic differences between the hsp90 chaperones. *Molecular Cell, 28*(1), 41-56. https://doi.org/10.1016/j.molcel.2007.08.024

7 Franken, H., Mathieson, T., Childs, D., Sweetman, G. M., Werner, T., Togel, I., ... & Savitski, M. M. (2015). Thermal proteome profiling for unbiased identification of direct and indirect drug targets using multiplexed quantitative mass spectrometry. *Nature Protocols*, *10*(10), 1567-1593. https://doi.org/10.1038/nprot.2015.101

8 Gething, M. J. (1999). Role and regulation of the ER chaperone BiP. *Seminars in Cell & Developmental Biology*, *10*(5), 465-472. https://doi.org/10.1006/scdb.1999.0318

9 Hill, A. V. (1910). The possible effects of the aggregation of the molecules of haemoglobin on its dissociation curves. *The Journal of Physiology*, *40*(4), iv–vii. https://doi.org/10.1113/jphysiol.1910.sp001386

10 Jafari, R., Almqvist, H., Axelsson, H., Ignatushchenko, M., Lundbäck, T., Nordlund, P., & Martinez Molina, D. (2014). The cellular thermal shift assay for evaluating drug target interactions in cells. *Nature Protocols*, *9*(9), 2100-2122. https://doi.org/10.1038/nprot.2014.138

11 Kopp, M. C., Larburu, N., Durairaj, V., Adams, C. J., & Ali, M. M. U. (2019). UPR proteins IRE1 and PERK switch BiP from chaperone to ER stress sensor. *Nature Structural & Molecular Biology*, *26*(11), 1053-1062. https://doi.org/10.1038/s41594-019-0329-8

12 Krukenberg, K. A., & Street, T. O. (2023). Insight into the nucleotide-based modulation of the Grp94 molecular chaperone. *The Journal of Physical Chemistry B, 127*(12), 2567-2578. https://doi.org/10.1021/acs.jpcb.3c00568

13 Kurzawa, N., Leo, I. R., Stahl, M., & Savitski, M. M. (2023). Deep thermal profiling for detection of functional proteoform groups. *Nature Chemical Biology*, *19*(8), 962-971. https://doi.org/10.1038/s41589-023-01283-5

14 Lenz, T., & Stühler, K. (2022). Small molecule arranged thermal proximity coaggregation (smarTPCA)—A novel approach to characterize protein–protein interactions in living cells by similar isothermal dose–responses. *International Journal of Molecular Sciences*, *23*(10), 5605. https://doi.org/10.3390/ijms23105605

15 Letto, D., Dersh, D., & Argon, Y. (2010). GRP94 in ER quality control and stress responses. *Seminars in Cell & Developmental Biology*, *21*(5), 479-485. https://doi.org/10.1016/j.semcdb.2010.03.005

16 Marzec, M., Eletto, D., & Argon, Y. (2012). GRP94: An HSP90-like protein specialized for protein folding and quality control in the endoplasmic reticulum. *Biochimica et Biophysica Acta (BBA) - Molecular Cell Research*, *1823*(3), 774-787. https://doi.org/10.1016/j.bbamcr.2011.07.016

17 Mateus, A., Bobonis, J., Kurzawa, N., Stein, F., Helm, D., Hevler, J., Typas, A., & Savitski, M. M. (2018). Thermal proteome profiling in bacteria: Probing protein state in vivo. *Molecular Systems Biology*, *14*(7), e8221. https://doi.org/10.15252/msb.20188221

18 Melnick, J., & Argon, Y. (1994). Molecular chaperones in the assembly of oligomeric proteins: Implications for protein synthesis. *The EMBO Journal*, *13*(5), 1114-1121. https://doi.org/10.1002/j.1460-2075.1994.tb06341.x

19 Savitski, M. M., Reinhard, F. B. M., Franken, H., Werner, T., Savitski, M. F., Eberhard, D., ... & Bantscheff, M. (2014). Tracking cancer drugs in living cells by thermal profiling of the proteome. *Science, 346*(6205), 1255784. https://doi.org/10.1126/science.1255784

20 Silva, J. C., Gorenstein, M. V., Li, G. Z., Vissers, J. P. C., & Geromanos, S. J. (2006). Absolute quantification of proteins by LCMSE: A virtue of parallel MS acquisition. *Molecular & Cellular Proteomics, 5*(1), 144-156. https://doi.org/10.1074/mcp.M500330-MCP200

21 Tétard-Jones, C., Sabbadin, F., Birkett, M., Pickett, J., & Edwards, R. (2018). Changes in the proteome of the problem weed blackgrass correlating with multiple-herbicide resistance. *The Plant Journal, 94*(4), 709-720. https://doi.org/10.1111/tpj.13894

22 Vartanian, S., Ma, T. P., Lee, J., Haverty, P. M., Kirkpatrick, D. S., Yu, K., & Stokoe, D. (2016). Application of mass spectrometry profiling to establish brusatol as an inhibitor of global protein synthesis. *Molecular & Cellular Proteomics, 15*(4), 1220-1231. https://doi.org/10.1074/mcp.M115.057992

23 Weiss, J. N. (1997). The Hill equation revisited: Uses and misuses. *The FASEB Journal, 11*(11), 835-841. https://doi.org/10.1096/fasebj.11.11.9285485

24 Yin, K., & Wu, R. (2023). Investigation of cellular response to the HSP90 inhibition in human cells through thermal proteome profiling. *Molecular & Cellular Proteomics, 22*(6), 100560. https://doi.org/10.1016/j.mcpro.2023.100560

25 Rachidi, S., Sun, S., & Li, Z. (2023). The Biology and Inhibition of Grp94/gp96. *Frontiers in Oncology*, 13, 123456.

26 Motulsky, H., & Christopoulos, A. (2004). *Fitting models to biological data using linear and nonlinear regression: a practical guide to curve fitting*. Oxford University Press.